Pharmaspire

RESEARCH ARTICLE

Molecular docking analysis of substituted 2-(1-benzylpiperidin-4-yl)-5-phenoxy-1*H*-benzo[d] imidazole derivatives as acetylcholinesterase inhibitors for the management of Alzheimer's disease

Abhimannu Shome, Pooja A. Chawla

Department of Pharmaceutical Chemistry, ISF College of Pharmacy, Moga, Punjab, India

ABSTRACT

The loss of cholinergic neurons in the brain and hippocampus is the hallmark of Alzheimer's disease (AD). The hydrolyzing enzyme acetylcholinesterase (AChE) has been identified as a potential treatment for AD. One of the most significant scaffolds for AChE binding is benzyl piperidine, which is included in the medication donepezil. Along with benzimidazole, early investigations have also shown to significantly inhibit AChE. This study includes in designing of a hybrid of benzyl piperidine and benzimidazole as AChE inhibitors. The study revealed that **B24**, **A24**, and **B8** showed the highest blood–brain barrier (BBB) permeability and binding affinities (−11.4 kcal/mol, 11.0 kcal/mol, and 11.1 kcal/mol, respectively). All the chemicals behaved similarly in the binding pocket of AChE. These important interactions between residues include those between Trp86, Tyr341, Ser293, and others. To stop the BBB from penetrating, polar substitutions on more than two locations were also identified. However, compound **B24** is an exception. The series' most potent ligands may be further evaluated biologically.

KEY WORDS: Acetylcholinesterase, Alzheimer's disease, Benzimidazole, Benzyl piperidine, Molecular docking

INTRODUCTION

Alzheimer's disease (AD) is a specific brain disorder that may display symptoms comparable to dementia, whereas dementia is a medical illness in which the patient has cognitive impairment. Alois Alzheimer, a neurologist from southern Germany, came across a patient around the turn of the 19th century who displayed unintentionally abnormal behavior, short-term amnestic disease, along with disorientation and dysphasia. This particular neurodegenerative disease was given the name AD in honor of that German physician.[1,2] A scientific research found that one in every nine adults over the age of 65 had AD. AD is becoming a major concern for the elderly. A 2019 survey found that 50 million people globally suffer from AD.[3]

Address for Correspondence:
Prof. (Dr.) Pooja A. Chawla,
E-mail: pvchawla@gmail.com

Dementia does not cause AD, although it can cause dementia through affecting memory. A statistical study found that in 2022, 27% of persons (1.75 million). Acetylcholine (ACh) levels reducing and cholinergic neurons deteriorating in the hippocampus and cortical area are linked to the cholinergic hypothesis. The hydrolyzing enzyme acetylcholinesterase (AChE), which is situated at the neuromuscular junction, is in charge of breaking down ACh. The AChE enzyme has an ellipsoidal shape, 12 strands, and a combination of 14 helixes and -sheets. It also interacts with amyloid plaque in people with AD.[4] The primary role of AChE is to hydrolyze

Access this article online

Website: http://isfcppharmaspire.com

DOI: 10.56933/Pharmaspire.2023.15111

Date of Submission: 19 May 2023
Date of Revision: 29 May 2023
Date of Acceptance: 30 May 2023

ACh, leading to the termination of synaptic impulses.[5] The extracellular matrix's amyloid plaque interacts with the AChE enzyme's peripheral site.[6-8] The interaction between the AChE and A complex makes amyloid fibrils more toxic than they would be on their own. ACh is hydroxylated by AChE, which lowers the quantity of ACh and impairs synaptic transmission. AChE's peripheral anionic site contains aromatic residues that interact specifically with the substrate (ACh). The carboxylate ion of glutamic acid acts as a hydrogen bond acceptor, pulling the proton from the imidazole ring of histidine and then from the hydroxy group of serine. This results in an electron cloud that is rich in electrons and assaults the carboxy group of ACh. Serine forms a covalent link with ACh, causing it to split into its acetyl and choline components [Figure 1]. On the other hand, AChE is more effective in hydrolyzing ACh. Aromatic residues selectively interact with the substrate (ACh) at the peripheral anionic site of AChE. To attack the carboxy group of ACh, the carboxylate ion of glutamic acid pulls the proton from the imidazole ring of histidine, then pulls the proton from the hydroxy group of serine. This creates an electron cloud that is rich in electrons. A covalent bond between serine and ACh causes the acetyl portion of ACh to be broken while keeping the choline intact. To attack the carboxy group of ACh, the carboxylate ion of glutamic acid pulls the proton from the imidazole ring of histidine, then pulls the proton from the hydroxy group of serine. This creates an electron cloud that is rich in electrons. A covalent bond between serine and ACh causes the acetyl portion of ACh to be broken while keeping the choline intact. There are also several different hypotheses about neurodegeneration in AD, such as the amyloid hypothesis and the tau hypothesis. The amyloid hypothesis proposes that neurodegeneration is induced by the accumulation of neurotoxic plaquing of a transmembrane protein, amyloid precursor protein. A different way, in the case of the tau hypothesis, is made up of tangled neurofibrils that cause the separation of the cytoskeleton of neurons. Prior research has clearly shown the substantial inhibitory efficacy of N-benzyl piperidine and benzimidazole-containing drugs against AChE. A series of donepezil-like compounds were reported by Costanzo *et al.* in 2016 as AChE inhibitors. The synthetic molecule with the highest inhibitory efficacy against AChE was compound **1** ($IC_{50:}$ 0.043 μM).[9] Similar to this, Asadi *et al.* reported a series of AChE inhibitors that included hybrids of phthalimide and dithiocarbonate. With a corresponding IC_{50} of 4.6 μM, compound **2** was found to be the most effective.[10] Another team of researchers discovered the high AChE inhibitory efficacy of compounds containing benzyl piperidine in 2019. They discovered that compound **3** with a pyridine substitution had the highest potency, with an IC_{50} of 0.41 μM. In the case of benzimidazole, another interesting scaffold, earlier investigations also revealed strong inhibitory activity against AChE.[11] Hussain *et al.* have published a series of benzimidazole-based thiazole derivatives in 2022. With an IC_{50} of 0.10 μM, compound **4** had the greatest potency among the synthetic compounds.[12] Similarly, a series of potent AChE inhibitors containing benzimidazole was discovered in 2020, with compound **5** ($IC_{50:}$ 0.60 μM) being the most effective in the series[13] [Figure 2]. We created two series of ligands using the results of these earlier investigations. Series B has nitrogen linkers while series A has oxygen linkers. Furthermore, molecular docking and ADME investigations will be used to screen these ligands [Figure 3].

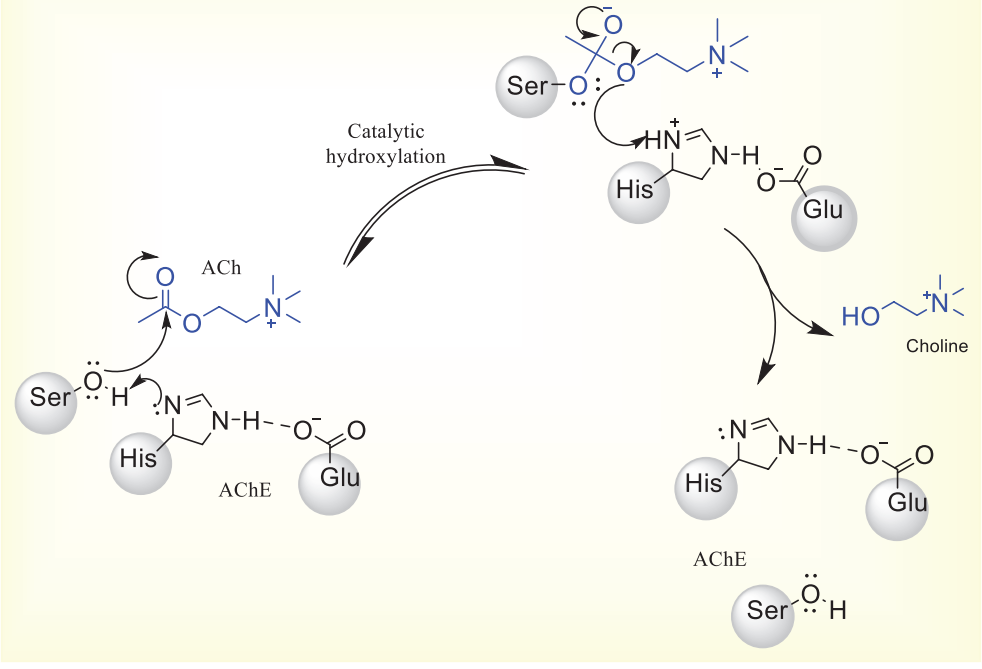

Figure 1: Catalytic break down mechanism of acetylcholine.

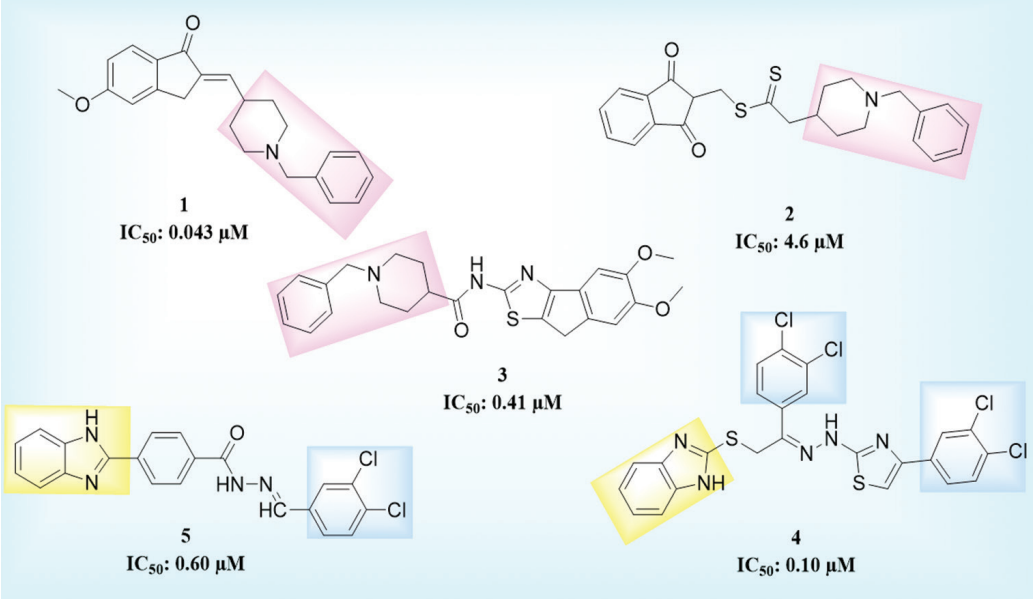

Figure 2: Literature survey of benzimidazole and benzyl piperidine containing acetylcholinesterase inhibitors.

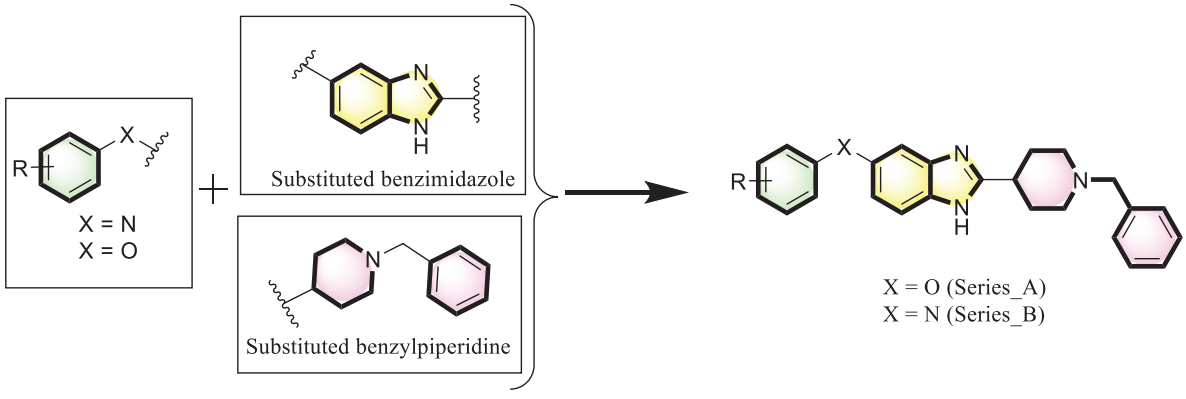

Figure 3: Rationale behind designing the new inhibitors.

MATERIALS AND METHODS

All the studies were performed on Dell Inspiron 15 3000 series with i3 10th Generation intel processor, 4 GB RAM, and 1TB ROM. The crystal structure of the AChE (PDB id. 4EY7) was obtained from the protein data bank for the computational study, that is, molecular docking.

Protein and ligand preparation

The crystal protein AChE was prepared in MGL tool 1.5.6. This process is comprised the deletion of the water molecule, addition of the partial kollman charge, and the addition of the polar hydrogens. In addition, grid generation was carried out on the donepezil's comparable binding site. Approximately, a grid dimension of 1Å with spacing of 24, 24, 24 along in x,y and z axis was developed. The proposed ligands were drawn using ChemDraw software. First, an MMFF94 force field with an RMS gradient of 0.001 was used to do the energy minimization in chem3d.[14] then.pdb format was stored. The final preparation was carried out in the next phase using MGL tool 1.5.6.[15,16]

Molecular docking

In Auto Dock Vina, a site-specific molecular docking study was carried out. A molecular docking tool based on the Lamarckian genetic algorithm produces nine docked conformations for each ligand.[17] The supramolecular association between the receptor and the ligand was optimized using this methodology, using a popular *in silico* technique, for the subsequent biological activity. Furthermore, these compounds were redocked and the RMSD was calculated to determine docking accuracy. In addition, the docking poses were observed in Discovery Studio to estimate the receptor-ligand contacts for activity.[18,19]

ADMET and drug-likeness prediction

ADMET and drug-likeness studies were performed to check the druggability of the designed compounds. This screening includes several parameters such as molecular weight (MW) (≤500 KDa), Log P (<5), hydrogen bond donor (HBD) (≤5), hydrogen bond acceptor (≤10), and topological polar surface area (TPSA) (≤120 [Å]^2) and number of rotatable bonds (<15). The drug-likeness and ADME prediction was performed on swissADME, a freeware webserver of Swiss Institute Of Bioinformatics.[20]

RESULTS AND DISCUSSION

Molecular docking studies

Molecular docking studies were performed in AutoDock Vina which showed a good fitting of the designed ligand inside the AChE binding cavity with similar interactions [Figure 4]. The volume of the AChE inhibitor binding pocket is approximately 910.91 Å^3 with a surface area of 734.09 Å^2. The main purpose of this docking study is to find out the optimal interactions between proteins and ligands. Those are necessary for the activity. The docking study was performed on AChE (PDB ID.4EY7). Total of nine conformations were generated by the software which was further visualized in discovery studio.

The proposed compounds interacted extensively with the AChE binding pockets, and the effects of HBDs and acceptors on the binding and the ADME profile were also seen. Particularly, the permeability of the blood–brain barrier (BBB) and GI absorption can alter depending on the location of halogen groups such as fluorine, bromine, and chlorine on the ring. Numerous substantial interactions that are comparable to the reference drug have also been reported. Compound **B24** had comparable interactions with several amino acids in the binding pockets in Figure 5, including Trp286, Trp86, Tyr337, and others, particularly on the peripheral site and the catalytic triad of Tyr341 and Ser293. Similar results occur when 3-methoxy substitution occurs [Figure 6], despite the fact that there are less hydrogen bonds. Only hydrogen bonding with Tyr72 was seen. However, it did exhibit negative interactions with Tyr124, Tyr341, and Trp286. When Tyr124 and Tyr72 were hydrogen bonded with 2,5-dimethoxy substituted derivatives, it also interacted with Trp286. In various regions of the compound skeleton, it showed a number of interactions between the π-cations and π-stacked with the ring's electron cloud [Figure 7]. For this investigation, donepezil was used as the standard, and it had a binding affinity of −10.6 kcal/mol.

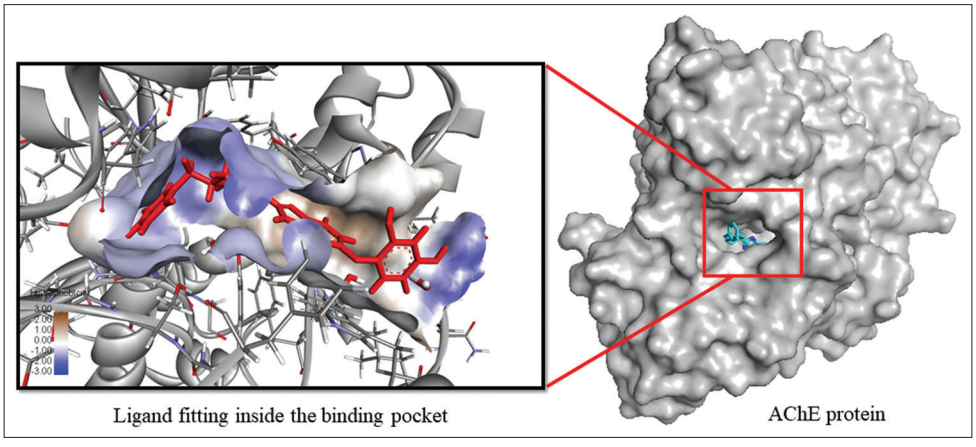

Figure 4: Ligand fitting inside the binding pocket of the acetylcholinesterase.

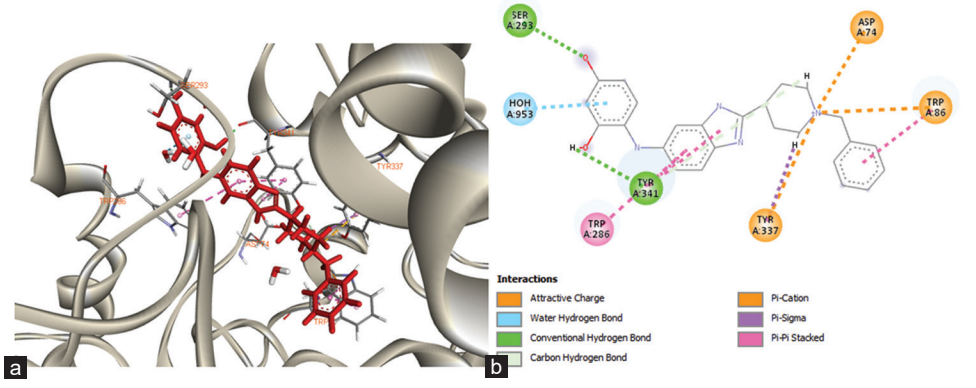

Figure 5: (a) 3D docking pose of B24 and (b) 2D docking poses of B24.

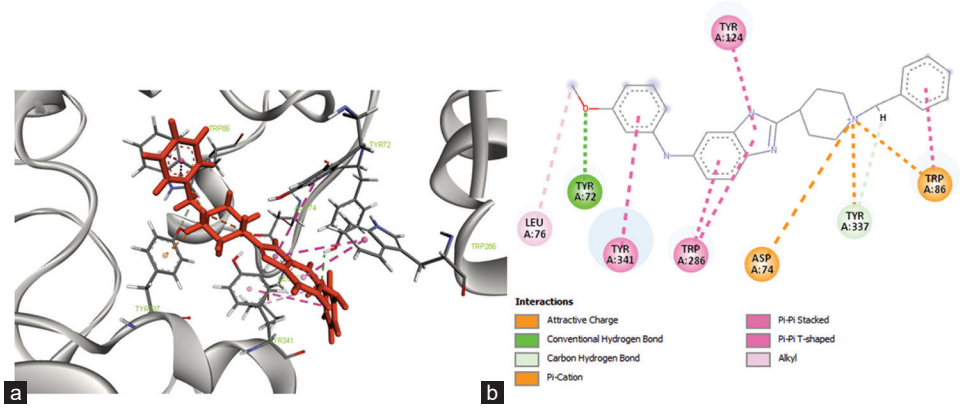

Figure 6: (a) 3D docking pose of B8 and (b) 2D docking pose of B8.

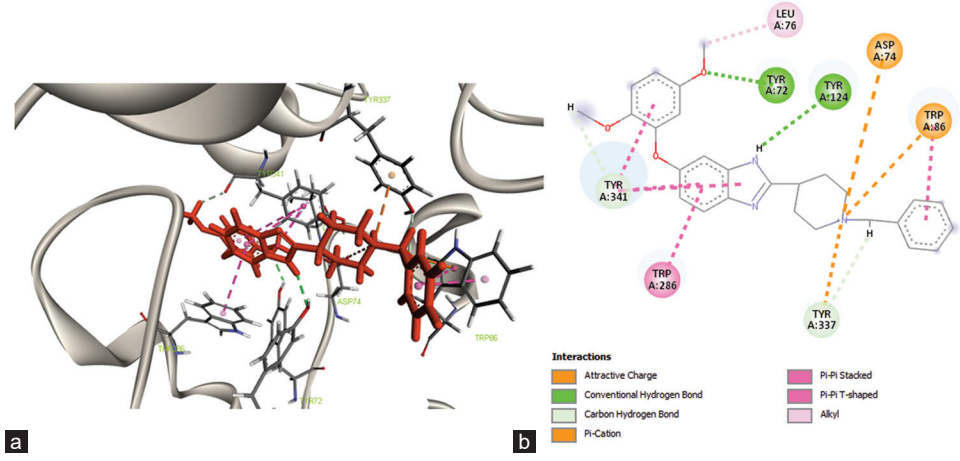

Figure 7: (a) 3D docking pose of A24 and (b) 2D docking pose of compound A24.

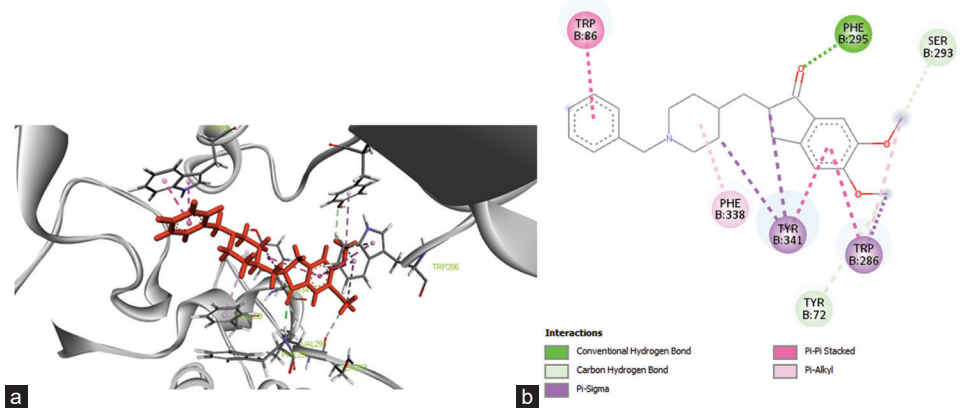

Figure 8: (a) 3D docking pose donepezil and (b) 2D docking pose of donepezil.

Comparatively to donepezil, compound **B24** had greater binding potency (−11.4 kcal/mol). It was evidently discovered that all binding modes were comparable to those of donepezil [Figure 8]. Particularly, the large, electron-rich amino acid residue Trp86 shows π-π interaction with the benzyl ring cloud. However, the interaction changed into a charge-attracted interaction as a result of the protonation of the nitrogen in the piperidine. However, the piperidine molecule must be protonated in order for the inhibitory action to occur. All of the compounds demonstrated greater accuracy in the redocking procedure, with significant RMSD <2Å. Despite the fact that, compound **B24** had a very low RMSD of 0.395Å. It validated the best fitting of the ligands as well as the reproducibility of the method and

the tool. All the interactions with their distance are shown in Table 1. Further, interacting residues along with distance and interaction types are shown in Table 2.

Drug-likeness and ADME

In the drug-likeness and ADME prediction, none of the compounds displayed any breaches of the Lipinski rule. All of the proposed ligands, with the exception of bromo, chloroma hydroxyl, and methoxy-modified molecules, demonstrated a considerable blood–brain barrier permeation due to their growing polarity. However, these phenomena can change depending on where the halogen and methoxy groups are located. The fluro group at the third position or the chloro group at the 2nd position was shown to have high BBB permeability. Compounds A10, A5, B5, and B10 are restricted from permeating the BBB due to a sharp rise in topological polar surface area (TPSA) caused by substitutions at the 2nd, 4th, and 6th positions with nitro or methoxy groups. However, BBB penetration also occurs in the case of molecules containing methoxy, particularly at the 2nd and 5th positions. No PAINs were detected for any of the compounds in the series, which strongly shows that these compounds are AChE-selective, as shown in Table 3.

A total of 48 ligands were developed and investigated in this *in silico* study using molecular docking, drug-likeness, and ADME. All of the compounds have been found to fit well into the AChE binding pocket and to interact similarly with donepezil. Here, the 2nd position of the benzimidazole was clubbed with benzyl piperidine, favoring a particular binding mode for optimum interactions. The 2nd scaffold, benzimidazole, is a substitute for the reference medicine (donepezil's 2,3-dihydro-1H-inden-1-one). Additionally, it revealed a number of π-π interactions within the binding pocket. The preferred substituted phenyl group at the peripheral position is crucial due to its special interaction with the peripheral portion of the receptor. Except for **B24**, any polar substitution, such as methoxy, hydroxy, and halogen groups at more than two positions, prevents the designed compounds from permeating the BBB, as shown in Figure 9.

Table 1: Docking score of the designed ligands

S. No.	Compound	Docking score (Kcal/mol)	RMSD (Å)	S. No.	Compound	Docking score (kcal/mol)	RMSD (Å)
1	**A1**	−10.0	1.030	26	**B1**	−10.6	0.876
2	**A2**	−10.3	0.970	27	**B2**	−10.9	1.690
4	**A3**	−10.3	0.890	28	**B3**	−10.8	0.967
5	**A4**	−10.7	1.390	29	**B4**	−9.68	1.695
6	**A5**	−10.7	0.961	30	**B5**	−9.7	1.234
7	**A6**	−10.3	0.858	31	**B6**	−10.6	1.250
8	**A7**	−9.68	0.341	32	**B7**	−11.0	1.045
9	**A8**	−10.6	0.850	33	**B8**	−11.2	0.459
10	**A9**	−10.05	0.943	34	**B9**	−9.41	0.966
11	**A10**	−9.01	0.918	35	**B10**	−10.9	0.999
12	**A11**	−10.1	1.852	36	**B11**	−10.48	0.983
13	**A12**	−10.7	1.496	37	**B12**	−10.2	0.876
14	**A13**	−10.9	0.978	38	**B13**	−10.3	0.988
15	**A14**	−10.2	0.982	39	**B14**	−10.3	0.973
16	**A15**	−10.9	0.985	40	**B15**	−10.8	0.997
17	**A16**	−10.6	0.825	41	**B16**	−10.03	0.987
18	**A17**	−9.65	0.973	42	**B17**	−10.6	0.991
19	**A18**	−4.96	0.991	43	**B18**	−10.8	0.769
20	**A19**	−6.31	0.973	44	**B19**	−9.09	0.697
21	**A20**	−10.61	0.893	45	**B20**	−10.3	0.799
22	**A21**	−10.99	0.769	46	**B21**	−10.5	0.891
23	**A22**	−10.6	0.937	47	**B22**	−10.9	0.769
24	**A23**	−11.0	0.971	48	**B23**	−10.6	0.893
25	**A24**	−11.2	0.360	49	**B24**	−11.4	0.395
				50	**Donepezil**	−10.6	0.197

Table 2: Interacting amino and their distance of top ligands

S. No.	Compounds	Interacting amino acids	Distance (Å)	Interaction category	Interaction type
1	**B24**	A: ASP74	5.55754	Electrostatic	Attractive Charge
		A: TYR341	1.69821	Hydrogen Bond	Conventional Hydrogen Bond
		A: TYR341	2.85692	Hydrogen Bond	Carbon Hydrogen Bond
		A: TRP86	4.72887	Electrostatic	π-Cation
		A: TYR337	4.31964	Electrostatic	π-Cation
		A: TYR337	2.67666	Hydrophobic	π-Sigma
		A: TYR341	3.63085	Hydrophobic	π-π Stacked
2	**B8**	A: TYR72	2.3062	Hydrogen Bond	Conventional Hydrogen Bond
		A: TRP86	4.53407	Hydrophobic	π-π Stacked
		A: TRP86	3.9188	Hydrophobic	π-π Stacked
		A: TRP286	4.37304	Hydrophobic	π-π Stacked
		A: TYR341	5.95992	Hydrophobic	π-π T-shaped
3	**A24**	A: ASP74	5.45508	Electrostatic	Attractive Charge
		A: TYR124	2.48594	Hydrogen Bond	Conventional Hydrogen Bond
		A: TYR341	2.39236	Hydrogen Bond	Carbon Hydrogen Bond
		A: TYR337	2.90247	Hydrogen Bond	Carbon Hydrogen Bond
		A: TRP86	4.71016	Electrostatic	π-Cation
		A: TYR337	3.93108	Electrostatic	π-Cation
		A: TYR341	3.94177	Hydrophobic	π-π Stacked
		A: LEU76	4.22667	Hydrophobic	Alkyl
4	**Donepezil**	B: SER293	3.55026	Hydrogen Bond	Carbon Hydrogen Bond
		A: TYR72	3.61665	Hydrogen Bond	Carbon Hydrogen Bond
		A: TYR341	3.9158	Hydrophobic	π-Sigma
		A: TYR341	3.93888	Hydrophobic	π-Sigma
		A: TRP286	3.68349	Hydrophobic	π-Sigma

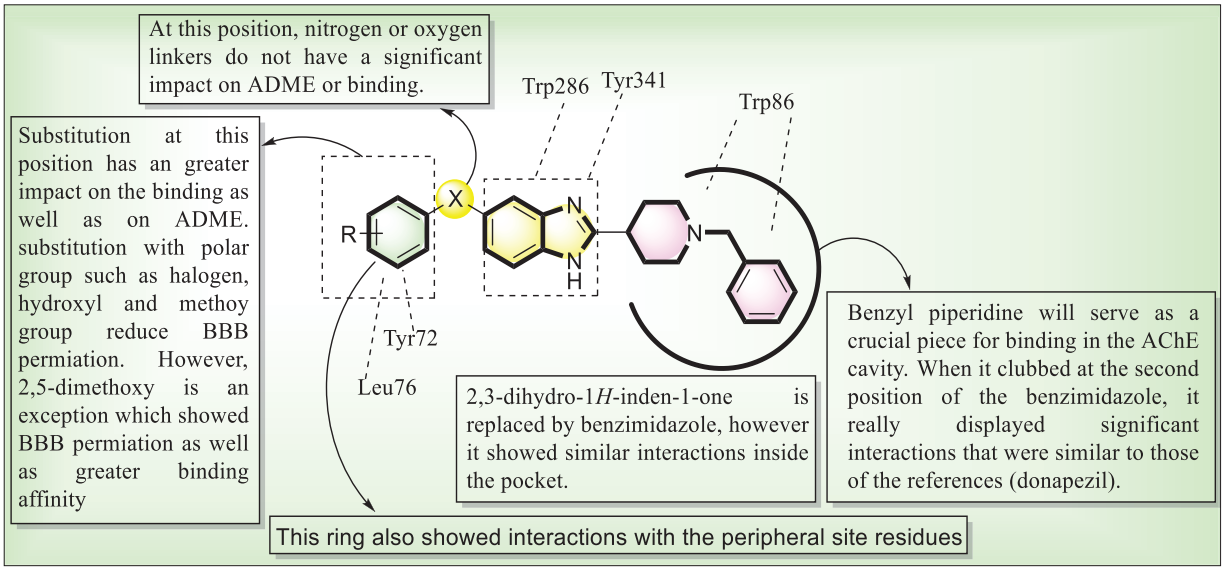

Figure 9: Correlation between structure and *in silico* screening results.

Table 3: Drug-likeness and ADME studies of the designed ligands

Compound	Substitutions	MW	HBD	HBA	Log P	TPSA (Å)^2	BBB	GI abs	Pains	Rotatable bonds	Lipinski Violations
A1	-	383.49	1	3	3.91	41.15	Yes	High	0	5	0
A2	-CH_3	397.51	1	3	4.11	41.15	Yes	High	0	5	0
A3	4-OH	399.48	2	4	3.35	61.38	Yes	High	0	5	0
A4	4-Cl	417.93	1	3	4.38	41.15	Yes	High	0	5	0
A5	2,4,6-Trinitro	518.48	1	9	2.13	178.61	No	Low	0	8	0
A6	4-OCH_3	413.51	1	4	3.55	50.38	Yes	High	0	6	0
A7	3,4-Dimethoxy	443.54	1	5	3.21	59.61	Yes	High	0	7	0
A8	3-OCH_3	413.51	1	4	3.55	50.38	Yes	High	0	6	0
A9	3,5-Dichloro	452.38	1	3	4.85	41.15	No	High	0	5	0
A10	2,4,6-trimethoxy	473.56	1	6	2.88	68.84	No	High	0	8	0
A11	Pyridine	384.47	1	4	2.87	54.04	Yes	High	0	5	0
A12	4-F	401.48	1	4	4.28	41.15	Yes	High	0	5	0
A13	2-Cl	417.93	1	3	4.38	41.15	Yes	High	0	5	0
A14	2,3-dimethoxy	443.54	1	5	3.21	59.61	Yes	High	0	7	0
A15	3-F	401.48	1	4	4.28	41.15	Yes	High	0	5	0
A16	3-Br	462.28	1	3	4.48	41.15	No	High	0	5	0
A17	2-NO_2	428.48	1	5	3.76	86.97	No	High	0	6	0
A18	3-Cl	417.93	1	3	4.38	41.15	Yes	High	0	5	0
A19	2-CH_3	397.51	1	3	4.11	41.15	Yes	High	0	5	0
A20	4-cyclopropyl	423.55	1	3	4.51	41.15	No	High	0	6	0
A21	3-OH	399.48	2	4	3.35	61.38	Yes	High	0	5	0
A22	3-OC_2H_5,4-OH	443.54	2	5	3.21	70.61	No	High	0	7	0
A23	2,4- dihydroxy	415.48	3	5	2.8	81.61	No	High	0	5	0
A24	2,5-dimethoxy	443.54	1	5	3.21	59.61	Yes	High	0	7	0
B1	-	382.5	2	2	3.91	43.95	Yes	High	0	5	0
B2	-CH_3	396.53	2	2	4.11	43.95	Yes	High	0	5	0
B3	4-OH	398.5	3	3	3.35	64.18	Yes	High	0	5	0
B4	4-Cl	416.95	2	2	4.38	43.95	Yes	High	0	5	0
B5	2,4,6-Trinitro	517.49	2	8	2.13	181.41	No	Low	0	8	0
B6	4-OCH_3	412.53	2	3	3.55	53.18	Yes	High	0	6	0
B7	3,4-Dimethoxy	442.55	2	4	3.21	62.41	Yes	High	0	7	0
B8	3-OCH_3	412.53	2	3	3.55	53.18	Yes	High	0	6	0
B9	3,5-Dichloro	451.39	2	2	4.85	43.95	No	High	0	5	0
B10	2,4,6-trimethoxy	472.58	2	5	2.88	71.64	No	High	0	8	0
B11	Pyridine	383.49	2	3	2.87	56.84	Yes	High	0	5	0
B12	4-F	400.49	2	3	4.28	43.95	Yes	High	0	5	0
B13	2-Cl	416.95	2	2	4.38	43.95	Yes	High	0	5	0
B14	2,3-dimethoxy	442.55	2	4	3.21	62.41	Yes	High	0	7	0
B15	3-F	400.49	2	3	4.28	43.95	Yes	High	0	5	0
B16	3-Br	461.40	2	2	4.48	43.95	No	High	0	5	0
B17	2-NO_2	427.5	2	4	3.76	89.77	No	High	0	6	0
B18	3-Cl	416.95	2	2	4.38	43.95	Yes	High	0	5	0
B19	2-CH_3	396.53	2	2	4.11	43.95	Yes	High	0	5	0
B20	4-cyclopropyl	422.56	2	2	4.51	43.95	No	High	0	6	0
B21	3-OH	398.5	3	3	3.35	64.18	Yes	High	0	5	0
B22	3-OC_2H_5,4-OH	442.55	3	4	3.21	73.41	No	High	0	7	0
B23	2,4- dihydroxy	414.5	4	4	2.8	84.41	No	High	0	5	0
B24	2,5-dimethoxy	442.55	2	4	3.21	62.41	Yes	High	0	7	0

CONCLUSION

AChE has consistently been identified as a key target for AD. Due to the severe loss of cholinergic neurons in the hippocampus region in brain results the depletion of acetyl choline (ACh) level. Similarly, AChE also a major cause of reduction of ACh level. One of the most crucial scaffolds for AChE binding is benzyl piperidine, which is also included in the medication donepezil. Along with benzimidazole, in which earlier investigations also showed considerable AChE inhibition. To create substituted 2-(1-benzylpiperidin-4-yl)-5-phenoxy-1H-benzo[d]imidazole derivatives and test their binding affinities and ADME profiles, benzyl piperidine and benzimidazole were combined in this work. The compounds **B24**, **A24**, and **B8** in this investigation had the greatest binding affinities as well as BBB permeability in the ADME analysis (-11.4 kcal/mol, 11.2 kcal/mol, and 11.2 kcal/mol, respectively). According to the docking accuracy data, compounds with higher affinity had an RMSD <1Å; however, rest of the compounds had an RMSD <2Å. In the AChE's binding pocket, all the compounds interacted similarly. These significant inter-residue interactions include Trp86, Trp286, Tyr341, Ser293, and others. Polar substitutions on more than two positions were also discovered to prevent the BBB from permeating. Compound **B24** is an exception, though. Compound **B24**, the most efficient chemical, will be employed in further biological tests.

ACKNOWLEDGMENT

The authors acknowledge the management of ISF College of Pharmacy for constant support.

CONFLICTS OF INTEREST

There are no conflicts of interest

REFERENCES

1. Bello-Lepe S, Alonso-Sánchez MF, Ortega A, Gaete M, Veliz M, Lira J, *et al.* Montreal cognitive assessment as screening measure for mild and major neurocognitive disorder in a Chilean population. Dement Geriatr Cogn Disord Extra 2020;10:105-14.
2. Prince MJ, Wimo A, Guerchet MM, Ali GC, Wu YT, Prina M. World Alzheimer Report 2015-The Global Impact of Dementia: An Analysis of Prevalence, Incidence, Cost and Trends; 2015.
3. Sauer J, Ffytche DH, Ballard C, Brown RG, Howard R. Differences between Alzheimer's disease and dementia with Lewy bodies: An fMRI study of task-related brain activity. Brain 2006;129(Pt 7):1780-8.
4. Neve RL, Harris P, Kosik KS, Kurnit DM, Donlon TA. Identification of cDNA clones for the human microtubule-associated protein tau and chromosomal localization of the genes for tau and microtubule-associated protein 2. Brain Res 1986;387:271-80.
5. Tapia-Rojas C, Cabezas-Opazo F, Deaton CA, Vergara EH, Johnson GV, Quintanilla RA. It's all about tau. Prog Neurobiol 2019;175:54-76.
6. Regan P, Piers T, Yi JH, Kim DH, Huh S, Park SJ, *et al.* Tau phosphorylation at serine 396 residue is required for hippocampal LTD. J Neurosci Res 2015;35:4804-12.
7. Yuzwa SA, Yadav AK, Skorobogatko Y, Clark T, Vosseller K, Vocadlo DJ. Mapping O-GlcNAc modification sites on tau and generation of a site-specific O-GlcNAc tau antibody. Amino Acids 2011;40:857-68.
8. Liu F, Shi J, Tanimukai H, Gu J, Gu J, Grundke-Iqbal I, *et al.* Reduced O-GlcNAcylation links lower brain glucose metabolism and tau pathology in Alzheimer's disease. Brain 2009;132:1820-32.
9. Costanzo P, Cariati L, Desiderio D, Sgammato R, Lamberti A, Arcone R, *et al.* Design, synthesis, and evaluation of donepezil-like compounds as AChE and BACE-1 inhibitors. ACS Med Chem Lett 2016;7:470-5.
10. Asadi M, Ebrahimi M, Mohammadi-Khanaposhtani M, Azizian H, Sepehri S, Nadri H, *et al.* Design, synthesis, molecular docking, and cholinesterase inhibitory potential of phthalimide-dithiocarbamate hybrids as new agents for treatment of Alzheimer's disease. Chem Biodivers 2019;16:e1900370.
11. van Greunen DG, van der Westhuizen CJ, Cordier W, Nell M, Stander A, Steenkamp V, *et al*. Novel N-benzylpiperidine carboxamide derivatives as potential cholinesterase inhibitors for the treatment of Alzheimer's disease. Eur J Med Chem 2019;179:680-93.
12. Hussain R, Ullah H, Rahim F, Sarfraz M, Taha M, Iqbal R, *et al*. Multipotent cholinesterase inhibitors for the treatment of Alzheimer's disease: Synthesis, biological analysis and molecular docking study of benzimidazole-based thiazole derivatives. Molecules 2022;27:6087.
13. Adalat B, Rahim F, Taha M, Alshamrani FJ, Anouar EH, Uddin N, *et al.* Synthesis of benzimidazole–based analogs as anti Alzheimer's disease compounds and their molecular docking studies. Molecules 2020;25:4828.
14. Ultra C. 6.0 and Chem3d Ultra. Cambridge, USA: Cambridge Soft Corporation; 2001.
15. Tool AD. 1.5.6 (ADT)/MGL Tools 1.5.6.California, USA: The Scripps Research Institute; 2016.
16. Huey R, Morris GM, Forli S. Using AutoDock 4 and AutoDock Vina with AutoDock Tools: A Tutorial. California, USA: The Scripps Research Institute Molecular Graphics Laboratory; 2012. p. 1000.
17. Li H, Leung KS, Wong MH, Ballester PJ. Improving AutoDock Vina using random forest: the growing accuracy of binding affinity prediction by the effective exploitation of larger data sets. Mol Inform 2015;34:115-26.
18. Studio D. Discovery Studio. Accelrys [21]; 2008.
19. Jejurikar BL, Rohane SH. Drug designing in discovery studio. Asian J Res Chem 2021;14:135-8.
20. Daina A, Michielin O, Zoete V. SwissADME: A free web tool to evaluate pharmacokinetics, drug-likeness and medicinal chemistry friendliness of small molecules. Sci Rep 2017;7:42717.